ONR Postdoctoral Fellowship Final Report: Geoacoustic Inversion and Source Localization in a Randomly Fluctuating Shallow Water Environment

Postdoctoral Fellow: Dr. Ying-Tsong Lin

MS#11, Woods Hole Oceanographic Institution, Woods Hole, MA 02543
phone: (508) 289-2329 fax: (508) 457-2194 email: ytlin@whoi.edu

Advisor: Dr. James F. Lynch
MS#11, Woods Hole Oceanographic Institution, Woods Hole, MA 02543
phone: (508) 289-2230 fax: (508) 457-2194 email: jlynch@whoi.edu

Award Number: N00014-08-1-0204

LONG-TERM GOALS

The long-term goal of this project is to understand and mitigate the uncertainties of shallow-water acoustic inversions caused by strong oceanic temporal and spatial variability. To achieve this goal, we need to investigate the connection between acoustic signal fluctuations and the water-column variability, and further incorporate this connection into the acoustic inversions for increasing the inversion performance.

OBJECTIVES

The scientific objectives of this project are centered on improving acoustic inversions for estimating bottom properties and source position in a randomly fluctuating shallow-water ocean. The first objective is to develop and test a new data nullspace projection method to suppress the inversion errors caused by the random water-column fluctuations. The second objective is focused on developing a source localization technique. The acoustic and oceanographic data collected from the SW06 experiment [1], a multi-disciplinary experiment sponsored by the ONR and conducted on the Mid-Atlantic Bight continental shelf in 2006, were used to test the developed technique and also to study how water column variability negatively affects source range estimates. In addition to the source localization work, the PI also developed an empirical orthogonal function (EOF) fitting method to merge different data to estimate the full water-column sound speed profiles in the SW06 experiment. The goal of this EOF fitting study is to provide a more complete oceanographic view of the local water-column variability to connect with the acoustic fluctuations seen in the data.

The 3D sound propagation effects of nonlinear internal waves are also studied in this project. Since the internal wave effect is one of the causes of acoustic signal variability seen in the data, it needs to be thoroughly investigated before we can develop an adequate scheme to reduce the inversion uncertainties caused by this effect.

APPROACH

The data nullspace projection method is the key method developed and used in this project to reduce the inversion uncertainties caused by random water-column fluctuations. The core of this method is to project the acoustic signals used for inversions onto a data nullspace that does not connect to the oceanic variability. In this way, the acoustic signal variations due to the water-column

REPORT DOCUMENTATION PAGE	*Form Approved* *OMB No. 0704-0188*

1. REPORT DATE *(DD-MM-YYYY)*	2. REPORT TYPE	3. DATES COVERED *(From - To)*
22-06-2010	FINAL	01/01/2008 - 12/31/2009

4. TITLE AND SUBTITLE	
Geoacoustic Inversion and Source Localization in a Randomly Fluctuating Shallow Water Environment	5a. CONTRACT NUMBER
	5b. GRANT NUMBER N00014-08-1-0204
	5c. PROGRAM ELEMENT NUMBER
6. AUTHOR(S) James F. Lynch and Ying Tsong Lin	5d. PROJECT NUMBER 130204sp
	5e. TASK NUMBER
	5f. WORK UNIT NUMBER

7. PERFORMING ORGANIZATION NAME(S) AND ADDRESS(ES)	8. PERFORMING ORGANIZATION REPORT NUMBER
Woods Hole Oceanographic Institution 98 Water Street Woods Hole, MA 02543	
9. SPONSORING/MONITORING AGENCY NAME(S) AND ADDRESS(ES)	**10. SPONSOR/MONITOR'S ACRONYM(S)**
Dr. Davis B. Reeder Office of Naval Research, Code 321 875 North Randolph Street Arlington, VA 22203-1995	ONR
	11. SPONSOR/MONITOR'S REPORT NUMBER(S)

12. DISTRIBUTION/AVAILABILITY STATEMENT
Approved for public release; distribution is unlimited

13. SUPPLEMENTARY NOTES

14. ABSTRACT
See Attached

15. SUBJECT TERMS

16. SECURITY CLASSIFICATION OF:			17. LIMITATION OF ABSTRACT	18. NUMBER OF PAGES	19a. NAME OF RESPONSIBLE PERSON
a. REPORT	b. ABSTRACT	c. THIS PAGE			James F. Lynch
					19b. TELEPHONE NUMBER *(Include area code)*
Unclassified	Unclassified	unclassified	Unlimited	16	508-289-2230

fluctuations can be suppressed, and the desired information about bottom geoacoustic parameters and source location contained in the acoustic signals can be distinctly exposed. Empirical orthogonal function (EOF) analysis is also utilized in this method to determine a set of orthonormal basis functions, the EOF modes, for decomposing the fluctuating acoustic properties in the water column. The reason for doing this is that the data nullspace can be enlarged, so that more useful information contained in the acoustic signals can be captured. To determine the data nullspace, a water-column kernel that relates the acoustic signal variations with the oceanic EOF modes is first derived from linear perturbation theory, and then the data nullspace can be obtained by applying singular value decomposition onto the water-column kernel matrix.

In addition to the projection method, a normal mode back-propagation approach has also been developed for passively localizing a remote sound source. The acoustic and oceanographic data collected from the SW06 experiment were used for testing this normal mode approach. In short, the approaches of nullspace projection and normal mode back-propagation taken in this project involve theory, numerical calculation and experimental data analysis. The detailed explanations of the techniques developed are described in the next section, along with the work accomplished.

The SW06 experiment provides excellent acoustic and oceanographic data for studying shallow-water acoustics. The acoustic data include continuous-wave and broadband signals covering a frequency range from 50 Hz up to 1k Hz in the low frequency acoustics component of the experiment. The signals were transmitted from towed and moored sources and received by hydrophone arrays. The techniques developed in this project are tested and implemented using the experiment data. Also, the extensive oceanography measurements will be utilized to better estimate the temporal and spatial statistics of the oceanic variability.

To study the 3D sound propagation effects caused by nonlinear internal waves. A three-dimensional normal mode solution is found to describe the sound field in the internal wave duct, and Huygens' Principle is adopted to calculate the radiation field from the termination of the duct when necessary. To handle a realistic environment, a computer code implementing a three-dimensional parabolic approximation in Cartesian coordinates [2] is employed.

The EOF fitting method developed in this project is to merge partial overlapping time series of ocean profiles into a single time series of profiles using empirical orthogonal function (EOF) decomposition with the objective analysis. This method can be used to handle internal waves passing two or more mooring locations from multiple directions, a situation where patterns of variability cannot be accounted for with a simple time lag. Data from one mooring are decomposed into linear combination of EOFs. Objective analysis using data from another mooring and these patterns is then used to build the necessary profile for merging the data, which is a linear combination of the EOFs. This method is applied to temperature data collected at a two vertical moorings in the New Jersey Shelf Shallow Water 2006 experiment.

WORK COMPLETED

The tasks completed this year are itemized below.

1. Development and improvement of the data nullspace projection method and applications onto geoacoustic inversions

A study has been done to show that the inversion result can be improved with the data nullspace projection to reach a better balance between the solution variance and resolution. In addition, an objective way is found to determine how many EOF modes should be used in the projection method so that we can greatly reduce the inversion uncertainties caused by the water-column fluctuations and yet maintain good inversion resolution. This method has applied onto two geoacoustic inversions using different inverse methods: perturbative inversion and Bayesian inversion. The completed work is summarized below.

1.1 Perturbative geoacoustic inversion with data nullspace projection

The acoustic data collected from the J-15 towed source experiment conducted by Dr. Kyle Becker (Appl. Res. Lab., Penn. State Univ.) in the SW06 experiment is being used in this project to invert for the bottom sound speed profile at the experiment site. The source, which transmitted continuous-wave tones at 50, 75, 125, and 175 Hz, was towed along radials toward and away from a vertical and horizontal hydrophone line array to create synthetic apertures. The horizontal wavenumbers of the propagating modes of the transmitted tones are estimated with a method briefed below. A vertical mode filter is first utilized to separate the acoustic propagating modes, and then the horizontal wavenumbers of each mode along the source track can be estimated from the first derivatives of the phase of the mode filter outputs (complex mode amplitude) with respective to the source-to-receiver range. The vertical mode functions used in the filter are calculated by the acoustic normal mode program KRAKEN [3] with the *in situ* water sound speed measurements on the vertical hydrophone line array and a bottom model provided by a previous study [4]. The resultant modal wavenumber estimates (shown in the Figure 1) are further averaged over the whole source track and used as the input data for the inversion.

EOF analysis is implemented on the *in situ* sound speeds measured on the vertical hydrophone line array. A set of dominative EOF modes is found to describe the water-column sound speed variations and to be used in the data nullspace projection method. Perturbative geoacoustic inversions with and without the data nullspace projection are performed. In both inversions, the water-column sound speed profile in the environmental background model is the average sound speed profile measured on the vertical hydrophone line array, and the model water depth is the average value of the true water depths along the source track, which mildly vary between 80 m and 83 m. Since the average sound speed profile at the receiver site is taken to represent the profiles along the source track, the environment background model has considerable water-column mismatch. As a result, the inversion without the projection can not converge due to the contamination from the water-column mismatch. The inversion with the projection, on the other hand, does converge, and the resultant bottom sound speed profile is shown in Figure 2, where one can see that a lower sound speed layer on the top of the sub-bottom section is resolved.

1.2 Bayesian geoacoustic inversion with data nullspace projection

A numerical simulation has been implemented to show the feasibility of using the data nullspace projection to improve Bayesian geoacoustic inversion. A linear internal wave model is used to generate a random internal wave field, and, after implementing EOF analysis, it is found that using three EOF modes is adequate to describe the random water-column fluctuations. A homogeneous bottom model is given in this test, which leads two bottom properties, sound speed and density, to be determined in the inversion procedure. A set of modal wavenumbers at four frequencies (50, 75, 125, and 175 Hz), complementary to the data collected in the J-15 towed source experiment of Dr. Kyle Becker, are calculated by the KRAKEN program. Without the data nullspace projection the inversion needs to determine five parameters; two of them are bottom parameters, and the rest are the water-column sound speed EOF coefficients. On the other hand, with the data nullspace projection only the two bottom parameters need to be determined. The inversion results are shown in the Figure 3, and one can see that the inversion with the data nullspace projection yields a maximum likelihood solution with a better agreement to the given ground-truth.

2. Normal mode back-propagation approach for low-frequency broadband sound source localization

Acoustic normal modes are orthogonal bases to decompose a sound pressure field, and they have significant frequency dependence below a few hundred hertz in a typical continental shelf area (water depth ~ 100 m). Hence to properly decompose a sound pressure field, one needs to implement a broadband normal mode decomposition/filtering. The normal mode back-propagation approach for source localization utilizes one of the important properties of normal modes — modal dispersion; for a given mode, its modal phase and group speeds are dependent on the acoustic frequency. In general, the first step of this method is to implement a broadband mode filter to obtain individual modal arrivals. The second step is to back propagate the modal arrivals with their own speeds at the different frequencies. Finally, the source range estimate is found where the back-propagated modes align with each other. Two source localizations using the SW06 data are implemented and briefed below.

2.1 SW06 experiment data analysis: U. Miami sound source localization

The normal mode approach described above has been tested by applying it to the acoustic data of known source position collected in the SW06 experiment. The sound source analyzed here is the U. Miami sound source (MSM), and it transmitted M-sequence phase encoded source signals at five different frequency bands (100, 200, 400, 800 and 1600 Hz) for nearly 4 weeks. In this work, the 100 Hz signal (25 Hz bandwidth) is selected. Every half an hour, a 1.5-min long transmission, which contained 36 identical M-sequence phase encoded signals, was emitted. With a matched filter, such encoded signals can be compressed, and a detailed modal arrival pattern is revealed, see an example shown in Figure 4(a). Further implementing a least squares mode filter gives us excellent estimates of modal arrivals, see Figure 4(b).

To back-propagate the modal arrivals received at the VLA, one needs to calculate the theoretical modal speeds along the propagation path. In doing so, an environmental model is first reconstructed for the MSM source localization in this SW06 data analysis — this model has 3 range-independent water-column sound speed patches, accurate bathymetry, and tidal levels from data. Note that the range-independent sound speed patches are constructed using the water temperature measurements from the three moorings evenly distributed along the 19.74 km propagation path. After reconstructing the environment, the normal mode arrivals are back-propagated using a 25-m range interval with their own theoretical speeds calculated every 150 m. Two assumptions are given: 2-D in-plane propagation and no mode-coupling. An eight-day long time series of source range estimates are shown in Figure 5. Every half an hour, 35 M-sequence pulses are analyzed and 35 range estimates are obtained. The average value and standard deviation of these estimates are plotted. The total mean range estimate is 19.74 km for these 8-days data, which is the same as the true distance, along with a standard deviation of 570 m.

2.2 SW06 experiment data analysis: Sei whale localization

Comparatively little is known about sei whale (*Balaenoptera borealis*) vocalizations and behavior, and, in particular, very few recordings have been made in their presence in the Northwest Atlantic. A large number of sei whale calls were unexpectedly collected during the SW06 experiment, which introduced the first evidence of sei whales in this shallow water region. Using the normal mode approach developed in this project, we are able to track the remote locations of these whales up to tens of kilometers. This part of work is a cooperative effort with Mr. Arthur E. Newhall at the Woods Hole Oceanographic Institution. See Figure 6 for an example of the whale tracking result.

3. Statistical merging of data sources to estimate full water-column sound speed in the SW06 experiment

A method for merging overlapping profile data sets into a single time series of profiles using an objective empirical orthogonal function (EOF) fitting technique has been developed. The method was applied to data from the SW06 experiment. The sound speed profiles that result specify conditions for 43 days from the sea surface to the seafloor at the main VLA site, as shown in Figures 7 and 8, and the resultant sound speed profiles allow reliable acoustic propagation modeling, mode decomposition, and beamforming.

4. 3-D acoustic effects caused by nonlinear internal gravity waves

In addition to the acoustic inversion work, the PI also studied one important consequence resulted from sound propagation through a nonlinear internal wave field, 3-D sound focusing and refraction.

4.1 Horizontal radiation of sound from the termination of an acoustic duct formed by nonlinear internal gravity waves

The horizontal, modal trapping of sound in an internal wave duct leads to a rather complicated horizontal eigenvalue problem to solve, due to the detailed shapes of the internal waves that form the duct. Also, the sound radiation from a real, irregular duct termination is not simple to be handled by a theoretical means. So, rather than addressing a complicated case, a simple duct model which will still show most of the physics associated with the ducting and radiation effects is first considered. This model has two homogeneous water-column layers (the sound speed in the upper layer is slightly faster), and a homogeneous bottom is assumed. Simplified internal waves with square waveforms and parallel wavefronts depress the water-column layer interface to a certain depth, and the acoustic duct formed by the waves abruptly terminates at some place where an open end is formed. A three-dimensional normal mode solution is found to describe the sound field in the duct, and then Huygens' Principle is adopted to calculate the radiation field. The result of a calculation example is shown in Figure 9, and the environment model settings are provided in the caption of the figure.

To handle a realistic environment, a computer code implementing a three-dimensional parabolic approximation in Cartesian coordinates [2] is employed. The result from a numerical simulation shows a radiation beam pattern with similar features suggested by the simplified analytic model described above.

4.2 Sound propagation in a curved nonlinear internal wave field

The PI and his collaborators have examined the sound propagation effects caused by curved nonlinear internal waves. The curved waves of our interest have mean lateral deviation of the internal wave duct by more than half the spacing between internal waves over an acoustic path, giving a transition from ducting to antiducting. Basic analytical and fully 3-D numerical models of sound propagation are employed, and it is found that, in such an internal wave field, lower modes are tended to escape from the curved duct, and, on the other hand, higher modes are trapped in the duct. The exact "cut-off" mode number for the trapping condition depends on the geometry of internal waves and sound source frequency. See Figure 10 for an example of 100 Hz sound propagation in a curved internal wave field with 45-km curvature.

RESULTS

Data nullspace projection and applications to geoacoustic inversions

The results drawn from the inversion work are summarized first. In theory, the data nullspace projection method utilizes the following two important properties of the EOF decomposition and the data nullspace.

A. Compactness of the EOF decomposition, which allows us to reduce the rank of the water column kernel matrix, so that the existence of the data nullspace is guaranteed, and its size will be large enough to expose most of the information about bottom geoacoustic parameters and source location contained in the acoustic data.
B. Orthogonality of the data nullspace to the column vectors of a kernel matrix, which allows us to suppress the acoustic data variations due to uncertain water-column fluctuations, so that the inversion results can be more accurate.

The result from the perturbative geoacoustic inversion using the modal wavenumber data shows that the data nullspace projection can take care of the unknown water-column mismatch in the environment background model. Without using the projection method, the inversion can not even converge. The simulation of Bayesian geoacoustic inversion also has promising result. With the data nullspace projection, the dimensions of the parameter space are reduced so that the inversion process speed can be improved, and more importantly a better solution is reached.

SW06 U. Miami sound source localization

We have found that that the small time-scale (< 2 min) variability in the source range estimates are due to nonlinear internal waves, as the peaks of the standard deviations perfectly correlate with nonlinear internal wave events, see Figure 5(a). In addition, because the water column moorings were separated by $\sim$10 km from each other and yielded a spatial Nyquist sampling rate of 20 km, the environmental model that is constructed from the mooring data may not properly describe the water-column variability of wavelength less than 20 km. As a result, the reconstructed environmental model has water column mismatch and causes the larger time-scale variability seen in the range estimates.

Sei whale localization

The ability to passively track calling sei whales in the SW06 region will enable a novel study of (1) the individual "distinctiveness" of sei whale downsweep calls and (2) the social context in which calling behavior takes place. Further collaboration to looking into this problem has been initiated with Dr. Mark Baumgartner of the Woods Hole Oceanographic Institution.

Statistical merging of data sources to estimate full water-column sound speed in the SW06 experiment

The EOF fitting method has general practicality, and its advantages are summarized here. It has been shown that the water layer structure measured by one partial depth system can be accurately preserved in the merged profiles at another location in a spatially stationary region. The arrival time differences of internal waves at the two locations can be systematically and automatically compensated for without knowing exact internal wave propagation speeds and directions, see an example shown in Figure 8. Finally, the merged profiles provide a more complete oceanographic view of the local water-column variability. This is beneficial to connecting the acoustic fluctuations with the environmental changes.

3-D sound propagation effects of nonlinear internal waves

For an acoustic source located in an internal wave duct and sufficiently far from the termination, some of the propagating sound may penetrate the internal wave "wall" at high grazing angles, but a fair amount of the sound energy is still trapped in the duct. Due to the curvature of the internal waves, the trapped sound may not be able to follow the duct, and we have found that some ducted energy may penetrate the curved duct and form intensive beams. Whispering gallery effects may also been seen when the source and receiver both are on the same side of the exterior area in a ducting environment. In a truncated wave situation, the trapped sound will propagate towards the termination, and the across-duct sound energy distribution at the termination is unique for each acoustic vertical mode. The sound radiating outward forms significant horizontal beams associated with individual vertical modes. From both the analytical expressions and numerical calculations we see complex horizontal interference patterns within the duct. Also, anomalous sound radiation fields, having mode-dependent patterns with strong azimuthal and temporal variability, are predicted at locations far from the termination of a truncated internal wave duct, even though there is no evidence of a ducting condition at those locations.

IMPACT/APPLICATIONS

The most important impact of this project is to increase the capability of underwater acoustic inversion and source localization techniques in a randomly fluctuating shallow-water ocean. Also, the data nullspace projection method developed in this project can in theory be applied to many sonar systems to reduce the effects of unavoidable environmental variability.

RELATED PROJECTS

This postdoctoral fellowship is under the supervision of Dr. James Lynch at Woods Hole Oceanographic Institution. The acoustic and oceanographic data used in this project are collected from the ONR sponsored SW06 experiment. The Investigators are also working with Dr. Timothy Duda to investigate the horizontal radiation of sound from the termination of an acoustic duct formed by nonlinear internal gravity waves.

REFERENCES

[1] A.E.Newhall, T.F. Duda, K. von der Heydt, J.D. Irish, J.N. Kemp, S.A. Lerner, S.P. Libertatore, Y-T Lin, J.F. Lynch, A.R. Maffei, A.K. Morozov, A Shmelev, C.J. Sellers, and W.E. Witzell, Acoustic and Oceanographic Observations and Configuration Information for the WHOI Moorings from the SW06 Experiment, WHOI Technical Report WHOI-2007-04 (May 2007)

[2] T. F. Duda, Initial results from a Cartesian three-dimensional parabolic equation acoustical propagation code, WHOI Tech. Rept., WHOI-2006-041 (2006).

[3] M. B. Porter, The KRAKEN normal mode program, SACLANTECN Memorandum SM-245 (SACLANT Undersea Research Centre, La Spezia, Italy, 1991).

[4] Y.-M. Jiang, N. R. Chapman and M. Badiey, "Quantifying the uncertainty of geoacoustic parameter estimates for the New Jersey self by inverting air gun data," J. Acoustic. Soc. Am. 121, 1879-1894 (2007).

PUBLICATIONS

Duda, T. F., Y.-T. Lin and J. F. Lynch, "Acoustic mode beam effects of nonlinear internal gravity waves in shallow water (A)," *J. Acoust. Soc. Am.*, 123, 3943 (2008). [published, non-refereed]

Lynch, J. F., Y.-T. Lin and A. Newhall, "Applying the data nullspace projection method to a geoacoustic Bayesian inversion in a randomly fluctuating shallow-water ocean (A)," *J. Acoust. Soc. Am.*, 123, 3589 (2008). [published, non-refereed]

Duda, T. F., J. F. Lynch, Y.-T. Lin, A. Newhall, H. Graber and M. Caruso, "The effects of non-linear internal wave curvature on acoustic propagation (A)," *J. Acoust. Soc. Am.*, 123, 3588 (2008) [published, non-refereed]

Lin, Y.-T, T.F. Duda and J.F. Lynch, "Acoustic mode radiation from the termination of a truncated nonlinear internal gravity wave duct in a shallow ocean area", *J. Acoust. Soc. Am.*, vol. 126, pp. 1752-1765 (2009) [published, refereed]

Lin, Y.-T, James F. Lynch, and Timothy F. Duda, "Investigation of the impact of water column variability on acoustic inversions in a shallow water ocean (A)", *J. Acoust. Soc. Am.*, vol. 125, pp. 2510 (2009) [published, non-refereed]

Newhall, A. E., Y.-T. Lin, J. F. Lynch, and M. F. Baumgartner, "Sei whale localization and vocalization frequency sweep rate estimation during the New Jersey Shallow Water 2006 experiment (A)", *J. Acoust. Soc. Am.*, vol. 125, pp. 2738 (2009) [published, non-refereed]

Lynch, J.F., Y.-T. Lin, T.F. Duda, A.E. Newhall, "Acoustic ducting, reflection, refraction, and dispersion by curved non-linear internal waves in shallow water", *IEEE J. Ocean. Eng.*, vol. 35, pp. 12-27 (2010) [published, refereed]

Lin, Y.-T., A.E. Newhall, T.F. Duda, P. Lermusiaux, "Merging multiple partial-depth data time series using objective empirical orthogonal function fitting", accepted by *IEEE J. Ocean. Eng.* (2010) [accepted, refereed]

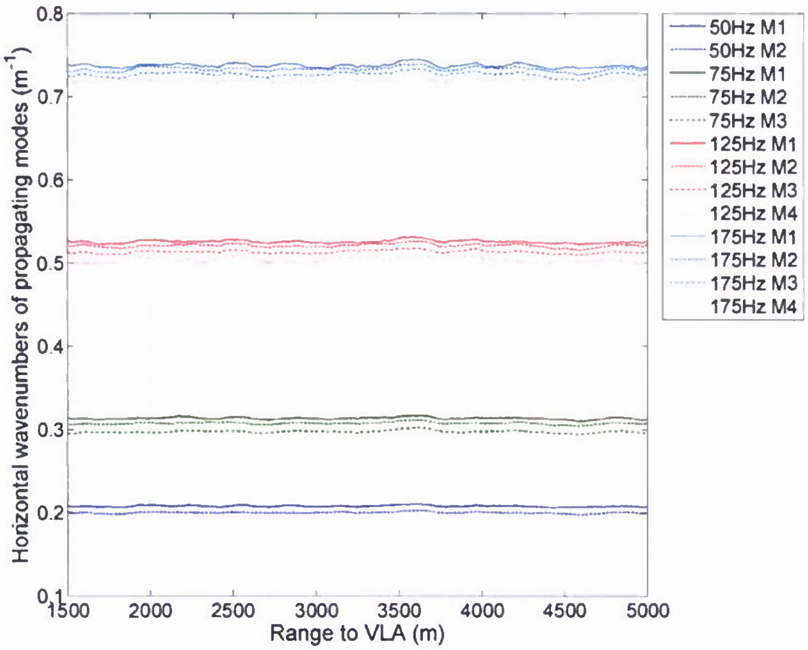

<u>Figure 1:</u> Modal wavenumbers estimates over the source track in the J-15 towed experiment

[Modal wavenumbers at four frequencies (50, 75, 125 and 175 Hz) are estimated from the continuous-wave tones transmitted by a towed source and received at a vertical hydrophone line array. Total 13 modes are analyzed; 2 modes at 50 Hz, 3 modes at 75 Hz, 4 modes at 125 Hz and 4 modes at 175 Hz. The variability seen in the data is caused by the environment complexity, including the spatially varying sediment properties and the spatial and temporal water-column fluctuations.]

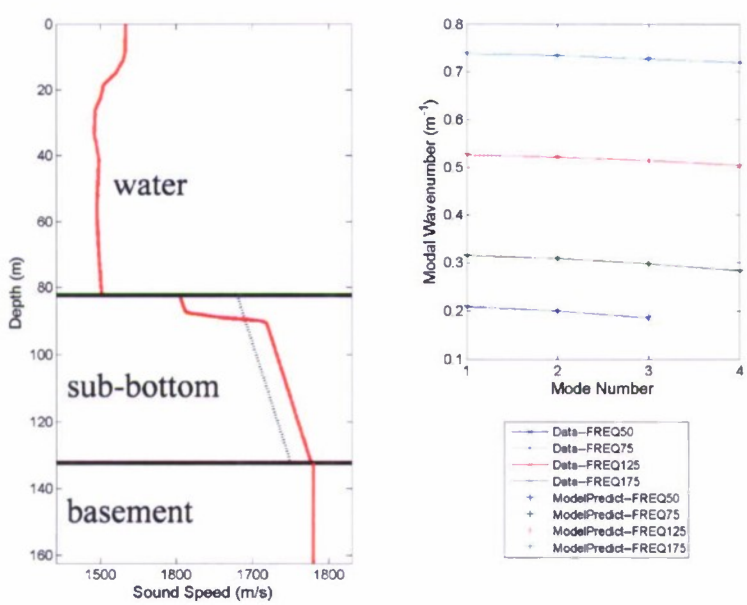

<u>Figure 2:</u> Inverted range-average bottom sound speed profile (left panel) at the J-15 towed source experiment site and the modal wavenumber data fitness (right panel)

[The water-column sound speed profile plotted here is the average profile measured on the vertical hydrophone line array during the experiment. The black dashed line shown in the sub-bottom section is the initial guess in the perturbative inversion procedure. One can see that a lower sound speed layer on the top of the sub-bottom section is resolved, and with the inverted bottom model the modal wavenumber predictions agree with the measured data very well.]

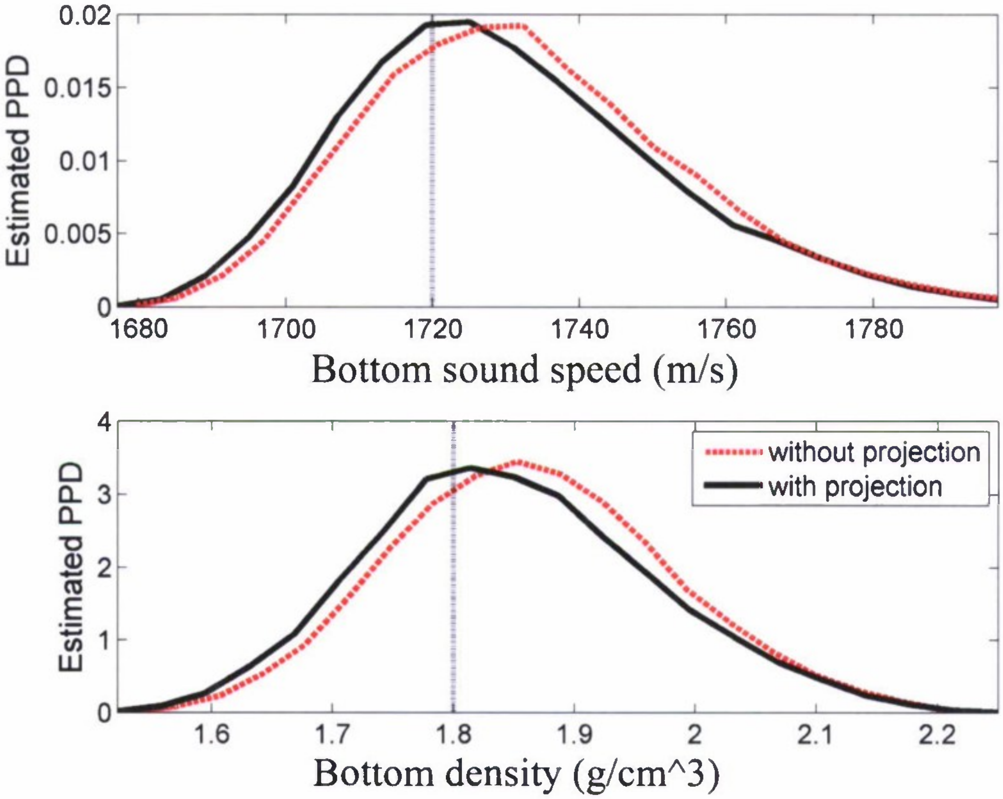

<u>Figure 3:</u> Numerical simulation results of Bayesian geoacoustic inversion in the presence of linear internal waves

[The vertical lines indicate the true sound speed and density in the homogeneous bottom. The simulation results suggest that the inversion with the data nullspace projection yields a maximum likelihood solution with a better agreement to the given ground-truth.]

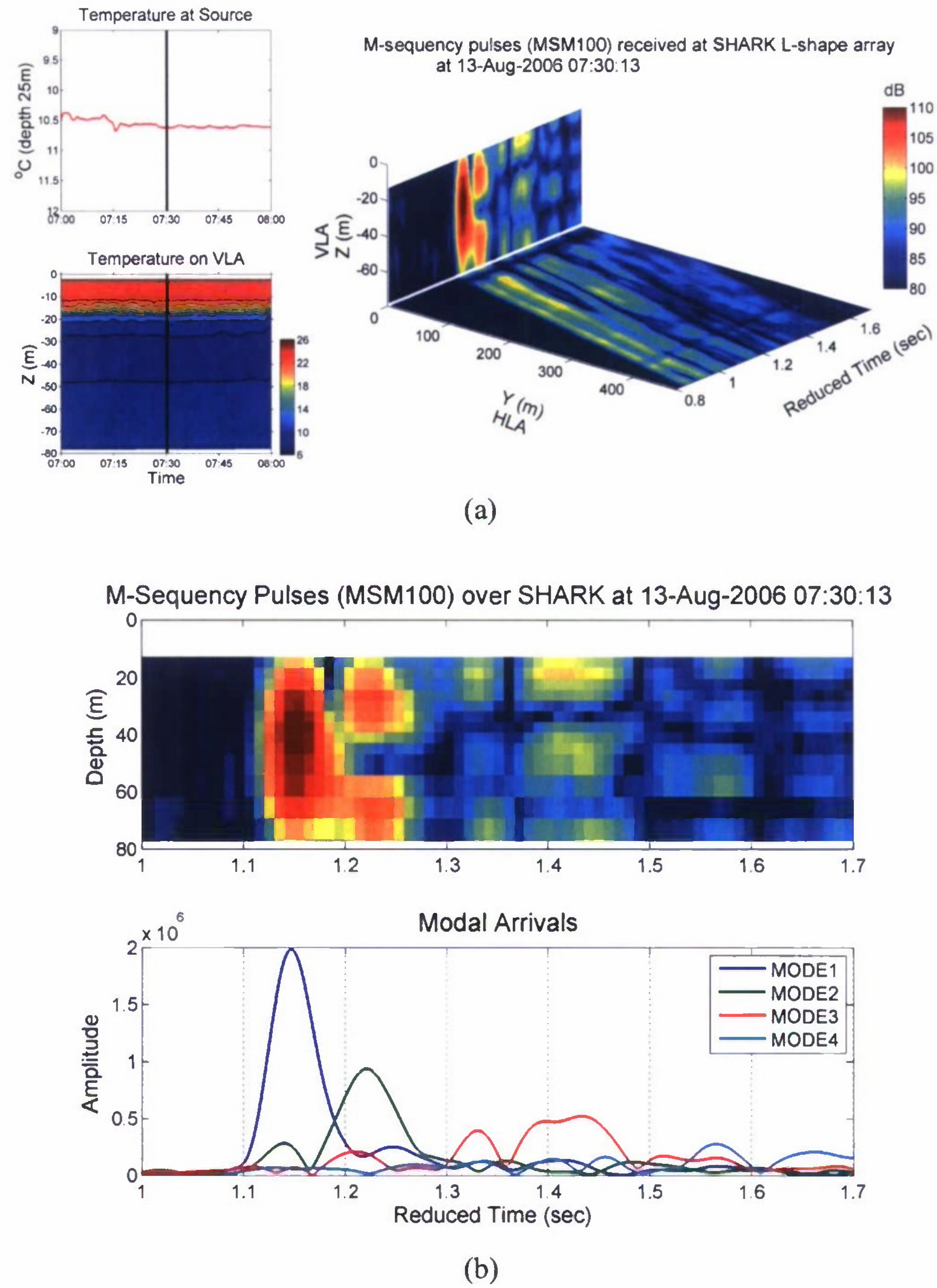

***Figure 4:** (a) An example of a 100-Hz M-sequence pulse reception and (b) detailed modal arrivals resulting from a least squares mode filter in the SW06 experiment*

[The M-sequence pulses were transmitted from the U. Miami sound source (MSM), which was located 19.74 km northeast (25.73° due North) away from the VLA. The compressed pulses are obtained from a matched filter. Using a least squares mode filter results in a clear modal arrival pattern.]

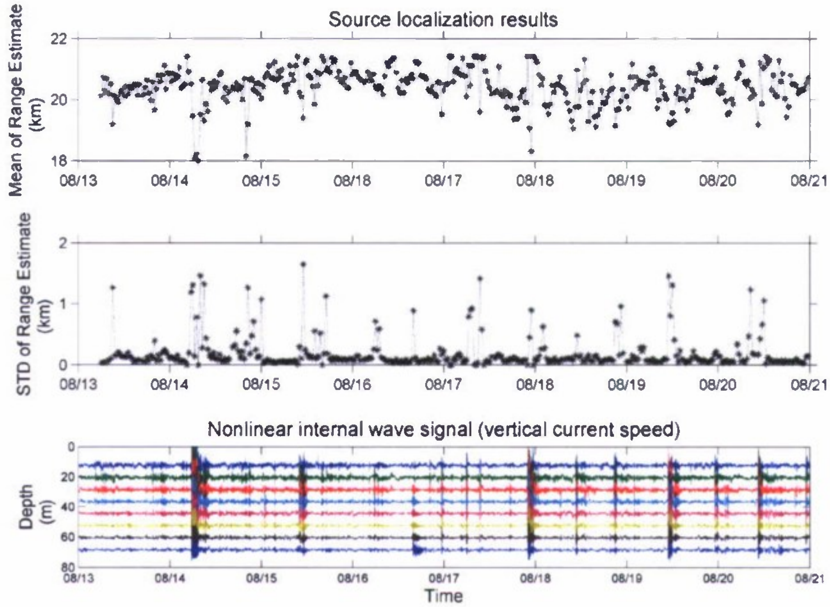

(a)

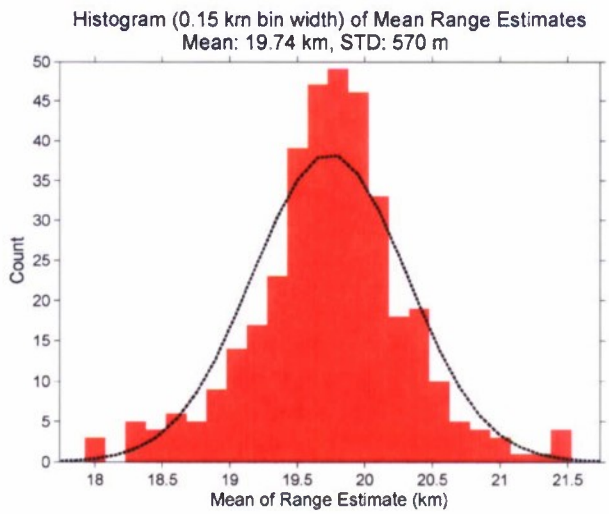

(b)

<u>Figure 5:</u> (a) The MSM source localization results and the nonlinear internal wave signal (vertical current speed) observed on the mooring in the middle of the propagation path. (b) Histogram of MSM source localization estimates.

[Panel (a) shows range estimates over 8 days. Every half an hour, 35 M-sequence pluses are analyzed and 35 range estimates are obtained. The average value and standard deviation of these estimates are plotted. The peaks of the standard deviations correlate with nonlinear internal wave events perfectly, indicating the waves are responsible to the short time-scale (< 2 min) variability. Panel (b) shows the histogram of the average range estimates. The total mean range estimate is 19.74 km for these 8-days data, which is the same as the true distance, along with a standard deviation of 570 m.]

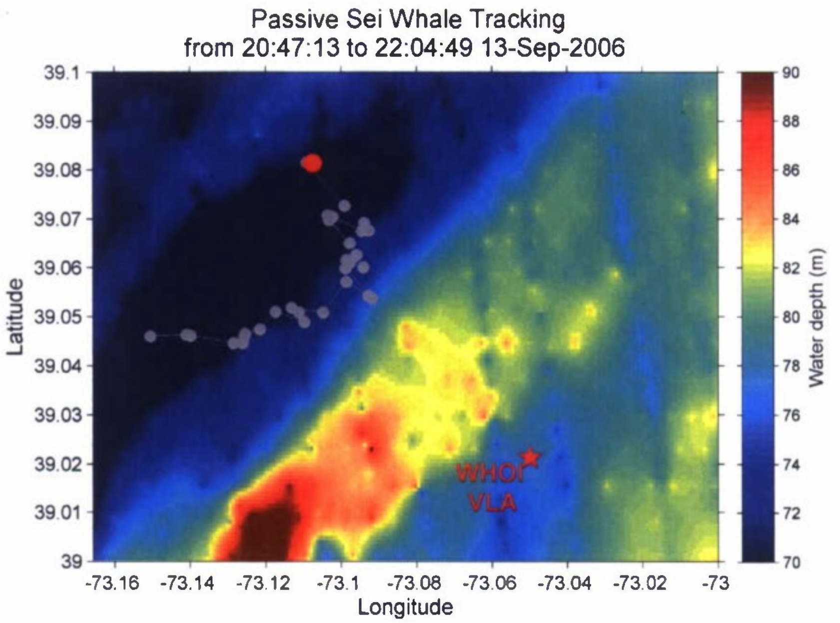

***Figure 6:* Estimated sei whale track from 22:47 to 22:05 on Sep 13 2006 in the SW06 experiment.**

[The red star is the position of the WHOI VLA/HLA and the dots are the whale locations. The red dot is the last whale location.]

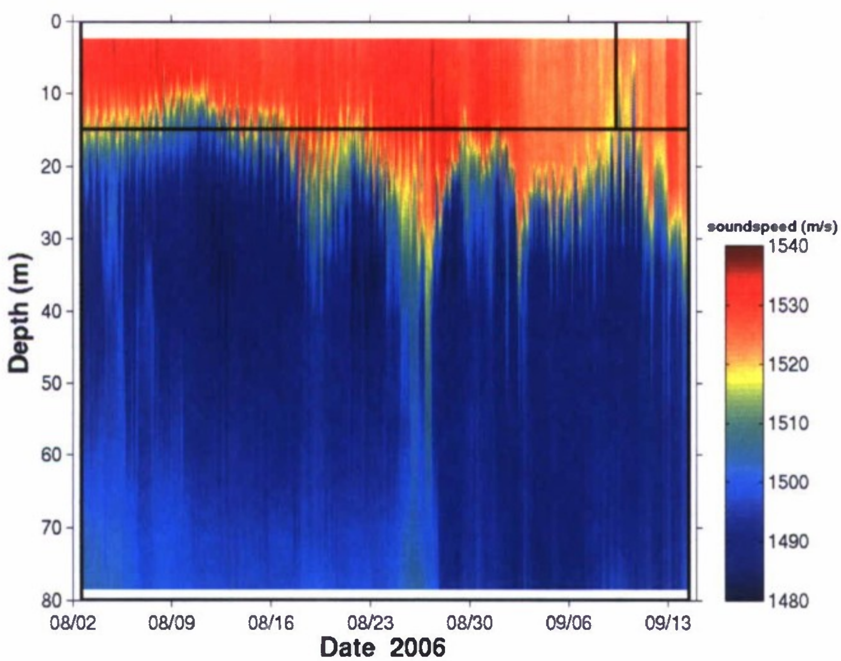

***Figure 7:* Full water-column sound speed profiles resulting from merging multiple data sources around and on the main VLA in the SW06 experiment.**

[Boxes identify areas of different temperature data sources. The upper left box indicates the ASIS surface buoy data, the upper right one is the MIT-MSEAS ocean model results and the lower big box is the WHOI VLA data. An additional data set from another nearby mooring is also used for incorporating salinity, along with some assistance from MSEAS ocean model results.]

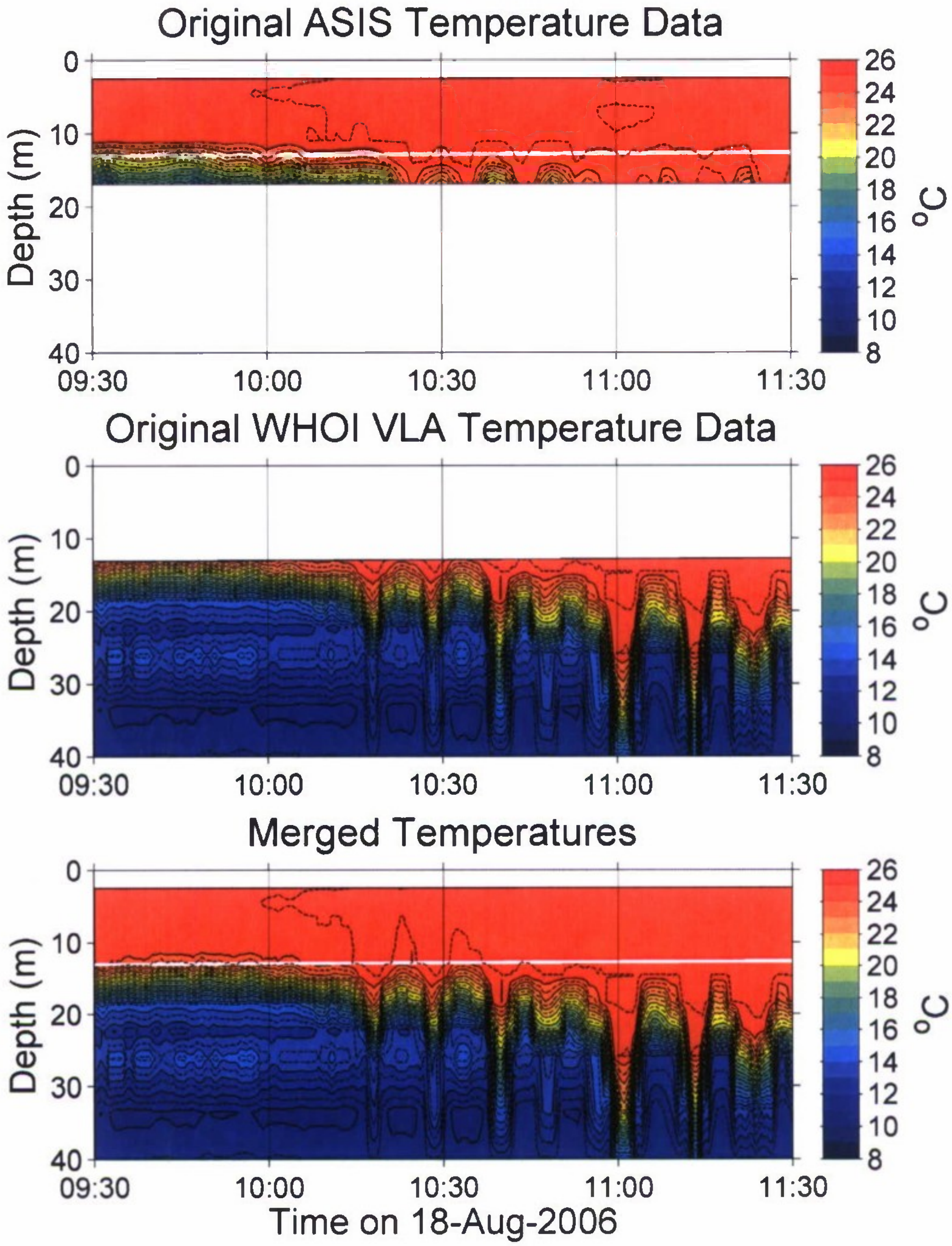

***Figure 8:** Contour plots of the original temperature data and the merged profiles during one large internal wave event in the SW06 experiment.*

[The objective EOF fitting technique developed in this project is utilized for the SW06 oceanographic data. This method preserves the mixed layer structure measured by the ASIS surface buoy in the merged profiles, and the arrival time differences of the nonlinear internal waves are automatically adjusted. Contour level increment is 1 degree in colors and 0.5 degree in lines.]

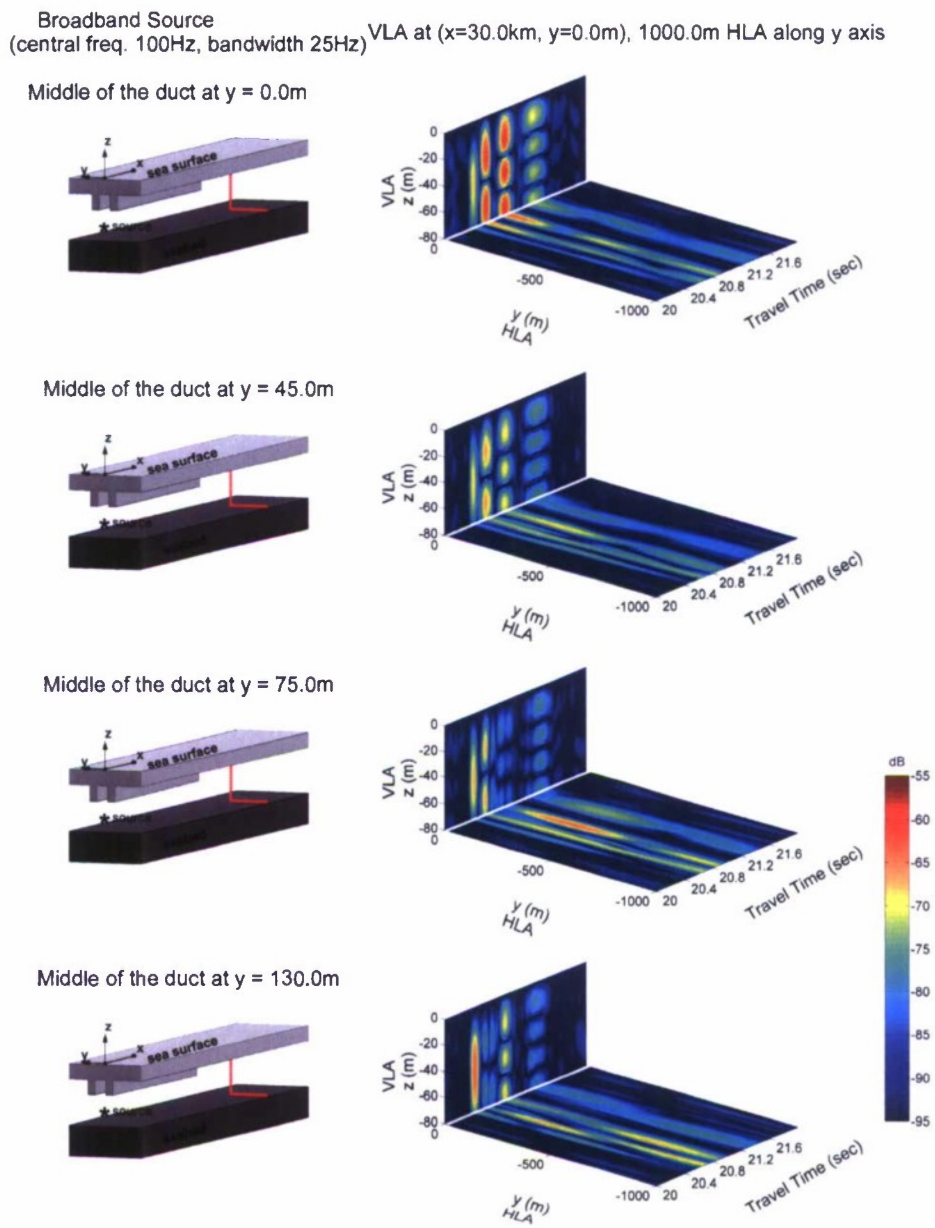

<u>Figure 9:</u> Analytical model of broadband sound radiation from the termination of a truncated internal wave duct

[The right panels illustrate the pulses received at a vertical and horizontal hydrophone line array, denoting by the red lines in the left panels, when the internal wave duct locates at four different positions. The broadband pulse is centered at 100 Hz with a 25 Hz bandwidth, and the environment model settings are detailed below. The sound speeds in the upper and lower water layers are 1,520 m/s and 1,480 m/s, respectively. The density in the water column (in both layers) is 1 g/cm^3. The water depth is 80 m, and the thickness of the upper water layer is 20 m. The amplitudes of the two internal square waves forming the acoustic duct are both 20 m, and their wavelengths are both 200 m. The gap between the internal waves is 300 m wide, and the internal waves abruptly terminate at x = 20 km. The sound speed and density in the homogeneous bottom are 1,700 m/s and 1.5 g/cm^3.]

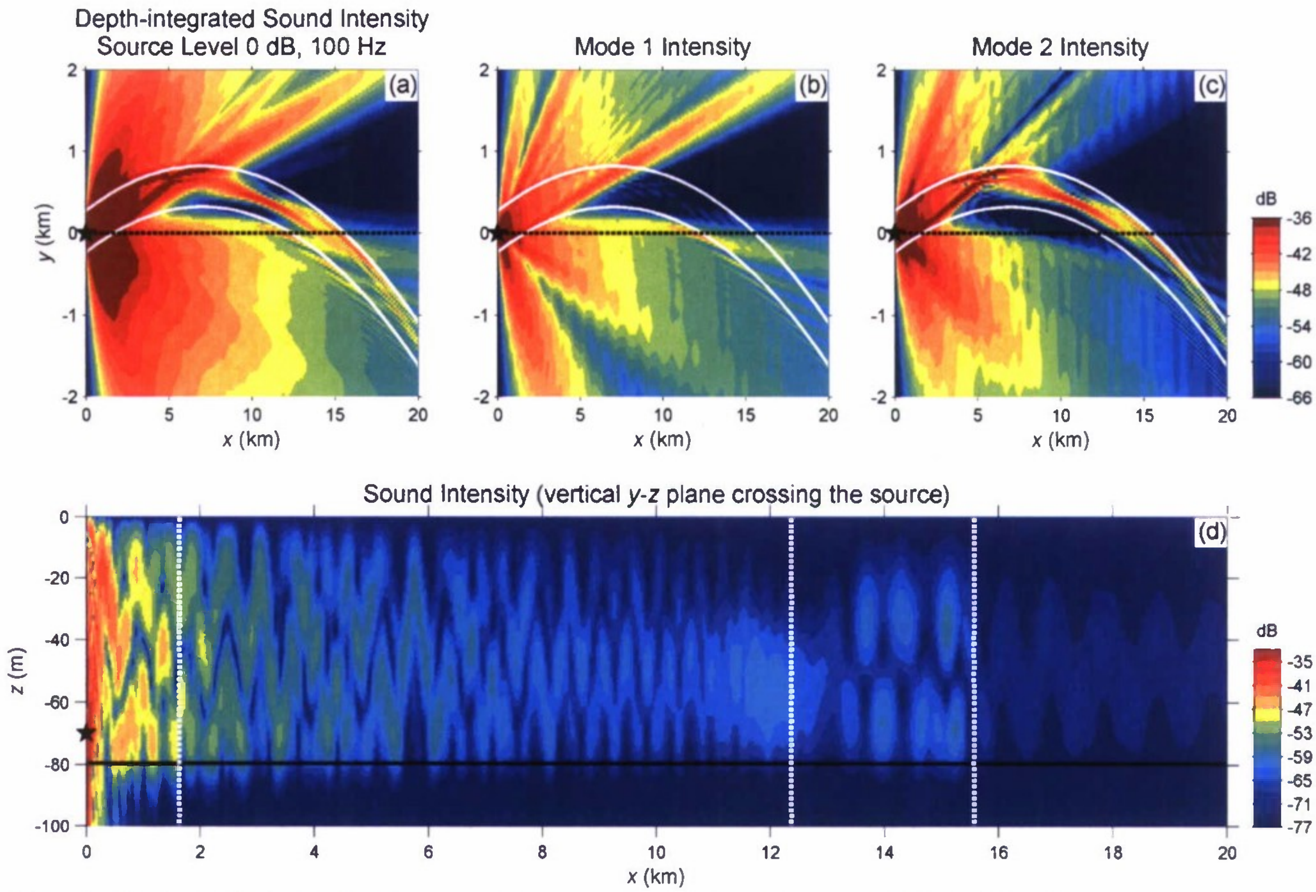

<u>Figure 10:</u> 100-Hz Sound propagation in a curved internal wave field. (a) Depth-integrated sound intensity. (b) Vertical mode 1 intensity. (c) Vertical mode 2 intensity. (d) Vertical slice of sound intensity at y=0 (all dB units are unity source level). The curvature of the internal waves is 45 km.

[In this numerical sound propagation model, we see both trapping and leakage of sound from the curved duct, as well as the initial escape of higher angle energy near the source. In panels b and c, we see that mode 1 is not trapped by the curved waveguide, but mode 2 is trapped by the curved duct, in accordance with our theory which predicts that higher modes trap better.]